Journal of Radioanalytical and Nuclear Chemistry (2019) 322:861–868
https://doi.org/10.1007/s10967-019-06727-y

Performance of biopolymer/graphene oxide gels for the effective adsorption of U(VI) from aqueous solution

Wei Peng[1] · Guolin Huang[1] · Shasha Yang[1] · Chenglun Guo[1] · Jeffery Shi[2]

Received: 25 June 2019 / Published online: 29 August 2019

Abstract
In exploration of an efficient and economical means for the treatment of radioactive wastewater, the performance of biopolymer/graphene oxide gels have been evaluated in the application for the separation of U(VI). The microscopic morphology and crystal structure of the obtained gels were analyzed by scanning electron microscopy, X-ray diffraction, Fourier transformed infrared spectra, and energy dispersive spectroscopy. The effects of adsorption factors such as solution pH and contact time were discussed to obtain the suitable process conditions. The experimental data were found to be agreed well with the Langmuri isotherm and the pseudo-second-order kinetic model.

Keywords Biopolymer · Uranium · Kinetics · Langmuir · Freundlich isotherm

Introduction

Uranium is the major resource for the nuclear power generation and such application represents a severe threat to the environment [1]. Currently, a number of methods have been focused on the treatment of these radionuclides from wastewater, such as chemical coagulation-flocculation, electrodialysis, precipitation, hydrogel membrane and adsorption [2–5]. Among these methods, adsorption technology has especially attracted significant attention due to its many advantages that are critical for commercialization, such as easy to operate and scale up, and high efficiency in removing U(VI) ions from aqueous solution [6, 7].

Graphene oxide (GO) is typical two-dimensional carbon nanomaterial containing unique structure and properties. Recently, it has become a hot topic due to its potential adsorption capacity of radionuclides [8]. However, the use of GO results in irreversible coagulation and impede the adsorption process and reduce the adsorption amount [9]. The GO-based materials with high adsorption capacity for U(VI) still presents a great challenge for the researchers. It is interesting to note that some published studies [10–14] have demonstrated that the biopolymers such as protein, DND, chitosan, and bovine serum albumin could graft onto the surface of GO and produce several adsorbents of sufficient stability for realizing effective removal of dye and heavy metals. It is worth researching the performance of the biopolymer mediated GO gels for the effective adsorption of uranium (VI).

In this study, a novel biopolymer/GO gels were prepared as effective adsorbents and applied to adsorption of U(VI) from aqueous solutions. The biopolymers selected in our study were bovine serum albumin (BSA) and sodium carboxymethyl cellulose (CMC). The adsorption performance of GO-BSA/CMC gels for the effective adsorption of U(VI) were evaluated by batch adsorption technique. The effects of pH value and contact time were discussed to obtain the optimum adsorption conditions. The kinetic, isotherms, and thermodynamic of adsorption process were also studied, and it will be critical for the sustainable development of nuclear energy and potential application for the removal of uranium (VI) from wastewater.

✉ Guolin Huang
guolinhuang@sina.com

[1] State Key Laboratory of Nuclear Resources and Environment, East China University of Technology, Nanchang 330013, China

[2] School of Chemical and Biomolecular Engineering, The University of Sydney, Sydney 2006, Australia

Materials and methods

BSA with a molecular weight of 66.446 kDa was purchased from Shanghai Lanji Biology Co., Ltd. CMC with a relative molecular weight of 263.2 was purchased from West Long Chemical Co., Ltd. The preparation of GO was based on the modified Hummers method. All other chemicals were of analytical-grade purity and used directly. The U(VI) solution was prepared by dissolving 1.1792 (±0.0001) g of U_3O_8 in 1000 mL of distilled water to form a U(VI) stock solution at concentration of 1 mg mL^{-1}, the method has been shown in Ref. [3]. Based on the reported literatures [15, 16], a lower initial U(VI) concentration is more desirable than a higher one for adsorption. Therefore, the initial concentration of U(VI) in this study was prepared at 100 mg mL^{-1} by diluting the stock solution.

A BSA stock solution was prepared by dissolving 0.1 g of BSA, 0.25 g EDCI, 0.1 g HOBT, and 0.05 g DMAP in 20 mL of deionized water, and stirred by using a 98-II-B magnetic stirring machine with temperature regulation (Changzhou, China) for 12 h to form 20% (w/w) BSA solution. 0.1 g of GO powder was dispersed in 20 mL of DI water/DMF (12/8, v/v) reaction mixture. The mixture was then added into the BSA stock solution, and sonicated for a few seconds in a FRQ-1002T ultrasonic wave cleaner (Hangzhou, China) to form a hydrogel. Finally, the hydrogel was freeze-dried in a FD-1A-50 freeze dryer (Yancheng, China) for overnight. The obtained product was denoted as GO-BSA gel in the paper.

A CMC stock solution was prepared by dissolving 0.4 g of CMC in 20 mL of deionized water, and stirred by a 98-II-B magnetic stirring machine with temperature regulation (Changzhou, China) for 30 min to form 2% (w/w) CMC solution. 0.1 g of GO powder was dispersed in 20 mL of the mixture of DI water/epichlorohydrin (18/2, v/v). The mixture was then added into the CMC stock solution, and sonicated for a few seconds in a FRQ-1002T ultrasonic wave cleaner (Hangzhou, China) to form a hydrogels. Finally, the hydrogel was freeze-dried in a FD-1A-50 freeze dryer (Yancheng, China) for overnight. The obtained product was described in the paper as GO-CMC gel.

Batch experiments of U(VI) adsorption were carried out by using the GO-BSA/CMC gels as the adsorbents in this study. Several erlenmeyer flasks along with 100 mg L^{-1} solutions of U(VI) and a known dosage of the adsorbents were shaken in a ZWYR-211D shaker (Zhengzhou, China) at 150 rpm and ambient temperatures for 3 h, which was adequate for reaching the equilibrium. The pH value was measured by a PHS-3C pH Meter (Hangzhou, China). The initial pH of each sample was adjusted until a constant pH with freshly prepared 0.5 mol L^{-1} H_2SO_4 or 0.5 mol L^{-1} NaOH. The batch technique has been shown in Ref. [3]. The suspensions were centrifuged and then a standard spectrophotometer method was used to analyse the concentration of U(VI) in the supernatant. Three replicates were used for each adsorption datum, and variation among these replicates found to be less than 2.5%. The adsorption capacity was determined by:

$$q_e = \frac{(C_0 - C_e)V}{W} \quad (1)$$

where C_0 and C_e are the initial and equilibrium concentrations of U(VI) in mg L^{-1}, respectively. V and W are the volume of U(VI) solution and the weight of the GO-BSA/CMC used, in L and g, respectively.

The characterization of prepared GO-BSA/CMC gels were measured by using the following instruments. The scanning electron microscopy (SEM) measurements were conducted on Nova Nano scanning electron microscopy 450 (FEI Co., Ltd., USA). X-ray diffraction (XRD) of the samples were measured by using D8-A25 (Bruker Instrument Co., Ltd., Germany). The Fourier transformed infrared spectra (FTIR) spectra of the samples were measured by using a Nicolet 380 FTIR spectrometer (Thermo Scientific Brand, USA) at room temperature. Energy dispersive spectroscopy (EDS) analysis was obtained by EX-250x (Horiba Co., Ltd., Japan).

Result and discussion

The surface morphologies of GO, GO-BSA and GO-CMC were demonstrated with SEM in Fig. 1. The wrinkle nanosheets are shown on the morphology in SEM image of GO. The thicker GO nanosheets and interconnected porous networks could be observed in the SEM images of GO-BSA/CMC compared to those in the pure GO. The results show that the distribution of biopolymer chains and GO plates is uniform. The interconnected pores make the diffusion of solute through the gels possible, which is extremely important for the potential applications for removal of U(VI).

XRD measurement was carried out to confirm the preparation of GO-BSA/CMC gels. As shown in Fig. 2, the peak that appear at 12.2° indicates the characteristic diffraction peak of crystalline structure of GO. In the XRD pattern of the GO-BSA, a broad and moderately strong peak located at the scope of 17°–25° is clearly seen. For the GO-CMC, the sharp peaks appear at 14.1° and 19.5° indicated the typical crystalline structure of cellulose. Meanwhile, in the XRD pattern of the GO-BSA/CMC gels, the diffraction peak at $2\theta = 12.2°$ in the GO gel disappears. These changes suggest that the transformation from GO to GO-BSA/CMC is accompanied successfully.

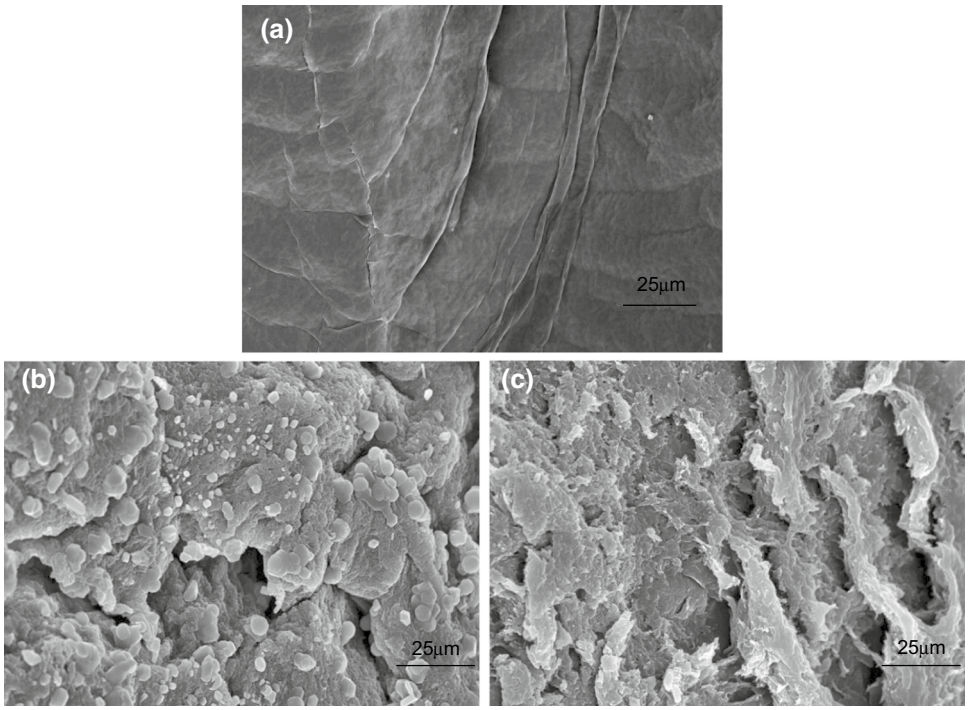

Fig. 1 SEM images of GO (**a**), GO-BSA (**b**) and GO-CMC (**c**)

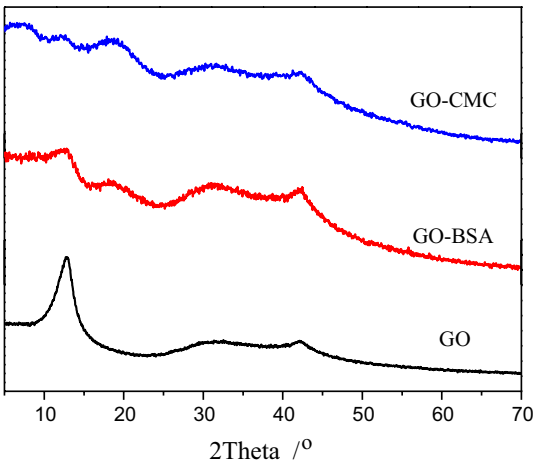

Fig. 2 XRD pattern of GO, GO-BSA and GO-CMC

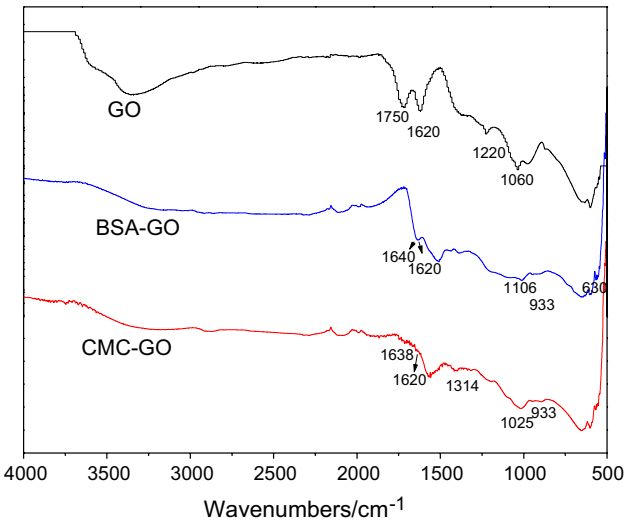

Fig. 3 FTIR spectra of GO, GO-BSA and GO-CMC

FTIR spectras of GO, GO-BSA and GO-CMC were also collected, as shown in Fig. 3. The pure GO shows characteristic peaks at 1750 cm^{-1} (C=O stretching of the carboxyl group), 1620 cm^{-1} (C=C stretching vibration of graphitic group), and 1220 cm^{-1} (C–O–C stretching of the epoxy) [11]. For the FTIR spectra of GO-BSA, a new band attributed to the in-plane bending vibration of O=C–NH appears at 630 cm^{-1} (which is not present in GO). Meanwhile, another new band appears at 1640 cm^{-1}, while the peak at 1750 cm^{-1} for pure GO disappeared, this is due to the cross-linking between amide groups and O=C–NH. These variations indicates the successful grafting of the amine groups of BSA onto GO [10]. For GO-CMC, the peaks at 1638 and 1025 cm^{-1} relate to the C=O and C–O–C stretching vibration, respectively. The peaks at 1314 cm^{-1} and 1620 cm^{-1} correspond to the stretching of C–N and C=N. These phenomenon indicate the successful formation of GO-BSA/CMC gels via crossing link.

The results of EDS analysis are shown in Fig. 4. It is observed that U(VI) ions had been adsorbed successfully onto the GO-BSA/CMC after adsorption. The possible mechanisms of adsorption process could be the cross-linking

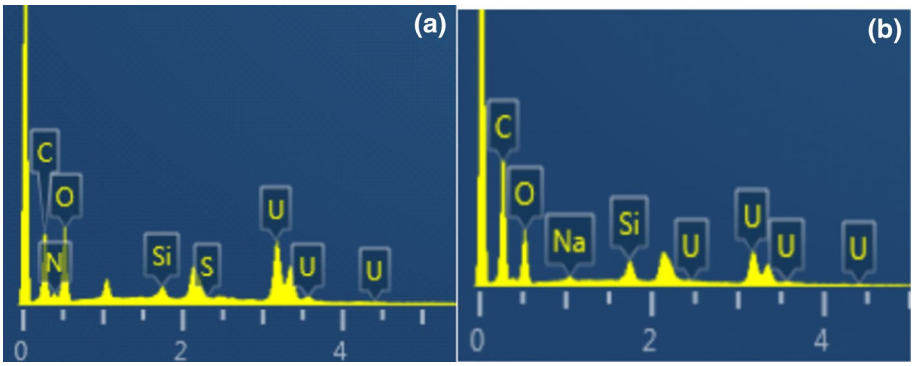

Fig. 4 EDS analysis of GO-BSA (**a**) and GO-CMC (**b**) after adsorption

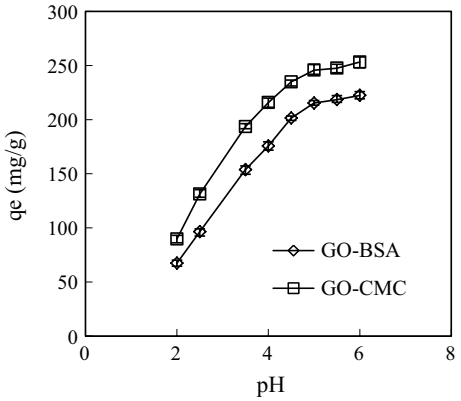

Fig. 5 Effect of pH on adsorption

reactions between the hydroxyl groups and BSA/CMC by hydrogen bonding and other interactions to U(VI) ions.

According to Fig. 5, the pH affects the adsorption capacity of U(VI) significantly at the pH range of 2.0–6.0, which is due to the variable speciation of uranium and adsorbent surface charge in different pH conditions. When the pH value of the solution increases from 2.0 to 5.0, the absorption amount of U(VI) increases gradually. As known, acidic solutions have a relatively high hydrogen ion concentration, which competed strongly with the positive uranium species including UO_2^{2+}, $UO_2(OH)^+$, and $(UO_2)_3(OH)^{5+}$ for the adsorption sites [3]. With increasing pH, the carboxylic and hydroxyl groups could be deprotonated to from $–COO^-$ and –O– groups, respectively. This could enhance the electrostatic attraction between the positive uranyl ions and the negative active groups on GO-BAS/CMC [13]. The maximum adsorption amount occurs at pH 5.0 at 298 K. The further increase of pH value will cause the precipitation of U(VI), the following experiments were carried out at pH 5.0.

Contact time also plays a major role in the adsorption, regardless of other experimental parameters, which affect adsorption kinetics. According to Fig. 6, when contact time increases from 20 to 120 min, the uptake capacity of U(VI) increases gradually and levels off at about 120 min in the temperature range studied, which was adequate for reaching

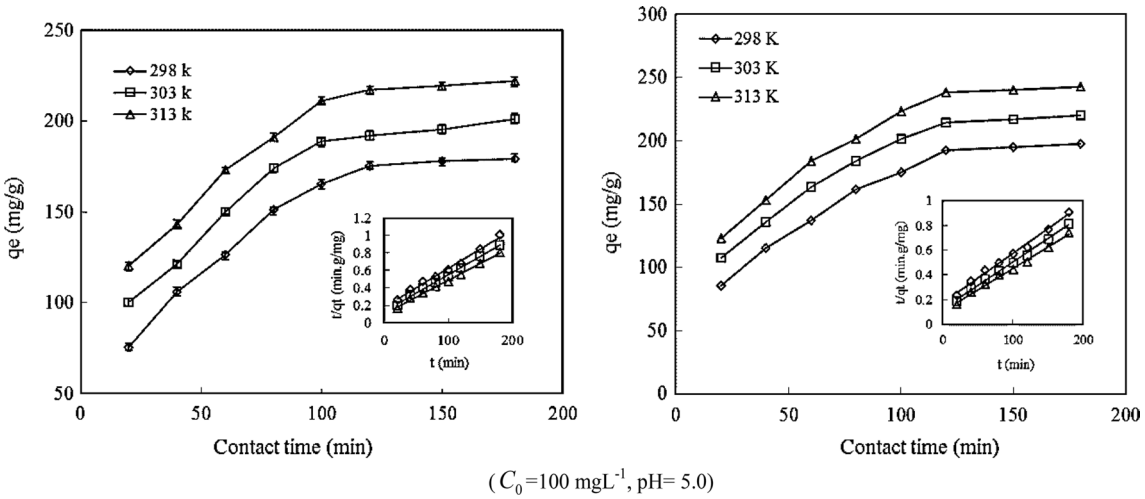

Fig. 6 Effect of Contact time on adsorption for GO-BSA (left) and GO-CMC (right). Inset shows the linearized pseudo-second-order plot

the equilibrium. There is no significant change from 120 to 180 min. Hence the following experiments were carried out at 120 min.

To determine the adsorption mechanism of U(VI) for GO-BSA/CMC gels, two kinetics models are used to assess the experimental data, i.e. the pseudo-first-order rate equation and the pseudo-second-order rate equation of Langergren. These two rate equations were determined as follows

$$\log(q_e - q_t) = -\frac{K_1 t}{2.303} + \log q_e \tag{2}$$

$$\frac{t}{q_t} = \frac{1}{q_e}t + \frac{1}{K_2 q_e^2} \tag{3}$$

where q_e and q_t are the U(VI) adsorption capacity at equilibrium and time t, in mg g^{-1}, respectively. K_1 and K_2 are kinetics constants, in L min^{-1} and g mg^{-1} min^{-1}, respectively.

The pseudo-first-order model ($Log(q_e–q_t)$ versus t, not shown) and the pseudo-second-order model (t/qt vs. t) are shown in the inset in Fig. 6, giving K_1, K_2, q_e and R^2 for the adsorption kinetics, and the obtained results are summarized and compared in Table 1.

Based on the correlation coefficient (R^2), the adsorptions of U(VI) for both GO-BSA and GO-CMC appear to be better fitted by the pseudo-second-order equation. The linearities are illustrated in the plots in the insets in Fig. 6 for the pseudo-second-order equation. The results implied that the adsorption processes might be chemisorption, which should be rate-limiting step. Similar result has been reported by Yang et al. [9].

The Langmuir and the Freundlich models are widely used to describe the equilibrium characteristics of the adsorption on a solid phase. These two isotherm models are expressed as

$$q_e = \frac{a_m K_L C_e}{1 + K_L C_e} \tag{4}$$

$$q_e = K C_e^{\frac{1}{n}} \tag{5}$$

where q_e is the U(VI) adsorption capacity of GO-BSA/CMC in mg g^{-1}. C_e is the concentration of U(VI) at equilibrium, in mg L^{-1}. The constants, a_m and K_L, are the maximum adsorption amount and the Langmuir adsorption constant, in mg g^{-1} and L mg^{-1}, respectively. Both K and $1/n$ are Freundlich constants related to the adsorption and intensity, in mL mg^{-1}, respectively.

The plots of C_e versus q_e of U(VI) on GO-BSA/CMC are showed in Fig. 7. The adsorption amount increased with higher equilibrium concentration and remained nearly saturation. The Langmuir isotherm (Ce vs. C_e/q_e) on GO-BSA/CMC for the adsorption process are plotted in the inset in Fig. 7. It is observed that Langmuir model describes the experimental data well, suggesting a monolayer coverage of U(VI) onto GO-BSA/CMC surface.

The isotherm parameters are showed in Table 2. Upon comparing the correlation coefficients, the Langmuir model was capable to simulate the adsorption process better (R^2 = 0.9974, 0.9947, 0.9959 for GO-BSA and R^2 = 0.9977, 0.9942, 0.9955 for GO-CMC) than Freundlich isotherm (R^2 = 0.9496, 0.9238, 0.91389 for GO-BAS and R^2 = 0.9553, 0.9549, 0.9746 for GO-CMC). The maximum adsorption capacity for U(VI) estimated from Langmuir isotherm at pH 5.0 and 313 K reaches 270.3 mg g^{-1} for GO-BSA and 322.6 mg g^{-1} for GO-CMC, respectively.

The essential characteristic of Langmuir model can be expressed by a separation factor R_L, which is described as the expression:

$$R_L = \frac{1}{1 + K_L C_0} \tag{6}$$

where C_0 is the initial concentration of U(VI) in mg L^{-1}. K_L is characteristic of Langmuir model, in L mg^{-1}.

The favorable adsorption process can be expressed when the value of R_L in the range from 0 to 1. In Table 2, The calculated values of R_L values (0.087–0.17) are less than 1, indicating the favourable adsorption of U(VI) ions onto GO-BSA/CMC.

Table 1 Simulation of kinetics data using the pseudo-first-order and pseudo-second-order models

Adsorbents	T (K)	$q_{e,exp}$ (mg/g)	Pseudo-first-order			Pseudo-second-order		
			$K_1 \times 10^2$ (L/min)	$q_{e,cal}$ (mg/g)	R^2	$K_2 \times 10^4$ (g/mg.min)	$q_{e,cal}$ (mg/g)	R^2
GO-BSA	298	179.3	3.54	332.5	0.9540	1.05	227.3	0.9926
	303	201.2	2.42	184.0	0.9765	1.32	238.1	0.9941
	313	222.4	3.10	253.0	0.9715	1.46	256.4	0.9954
GO-CMC	298	204.2	3.06	300.5	0.9428	0.93	250.0	0.9930
	303	225.5	2.86	265.1	0.9654	1.13	263.2	0.9956
	313	245.6	3.22	331.6	0.9378	1.14	285.7	0.9949

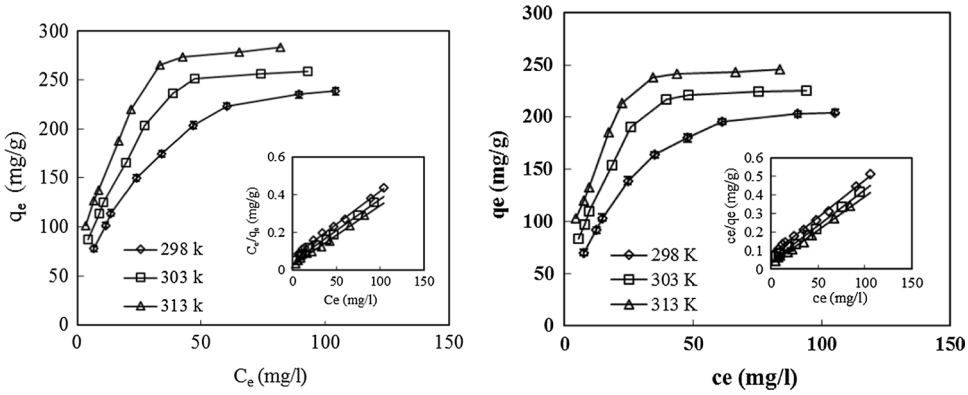

Fig. 7 Adsorption isotherm onto GO-BSA (left) and GO-CMC (right). The linear fitting of Langmuir model is shown in the inset figure

Table 2 Parameters of Langmuir and Freundlich models

Adsorb.	Temp. K	Langmuir isotherm				Freundlich isotherm		
		α_{max} mg g^{-1}	K_L L mg^{-1}	R^2	R_L	K mL mg^{-1}	n	R^2
GO-BSA	298	243.9	0.0533	0.9974	0.16	33.50	2.41	0.9496
	303	256.4	0.0892	0.9947	0.10	47.33	2.64	0.9238
	313	270.3	0.130	0.9959	0.071	67.25	3.08	0.9138
GO-CMC	298	285.7	0.0496	0.9977	0.17	37.27	2.37	0.9553
	303	303.0	0.0754	0.9942	0.12	50.62	2.56	0.9549
	313	322.6	0.105	0.9955	0.087	67.44	2.82	0.9746

Table 3 Comparison of the U(VI) adsorption capacity of various adsorbents

Material	Experiment conditions	Adsorption capacity (mg/g)	References
GO@sepiolite	pH = 5.0, T = 298 K, C_0 = 100 mg L^{-1}	161.3	[16]
GO@chitosan	pH = 5.0, T = 313 K, C_0 = 100 mg L^{-1}	204.1	[3]
GO@phosphate	pH = 4.0, T = 303 K, C_0 = 100 mg L^{-1}	251.7	[2]
GO@COOH	pH = 4.0, T = 293 K, C_0 = 100 mg L^{-1}	169.2	[8]
GO@manganese dioxide	pH = 6.0, T = 298 K, C_0 = 200 mg L^{-1}	185.2	[10]
GO@polyacrylamide	pH = 5.0, T = 313 K, C_0 = 100 mg L^{-1}	166	[15]
GO-BSA/CMC	pH = 5.0, T = 313 K, C_0 = 100 mg L^{-1}	270.3/322.6	This study

Table 3 shows the comparison of reported results which studies on the removal of U(VI) ions by different adsorbents. From Table 3, the adsorption amounts of GO-BSA/CMC nanostructure equal 270.3 mg g^{-1} and 322.6 mg g^{-1}, which exhibit higher adsorption capacities among these adsorbents, suggesting their superior characteristics as two effective adsorbents.

Thermodynamic parameters, including Gibbs free energy change ΔG^0 (in J mol^{-1}), enthalpy change ΔH^0 (in J mol^{-1}) and entropy change ΔS^0 (in J mol^{-1} K^{-1}) were evaluated and used to calculate the spontaneity and thermal properties of adsorption process. The thermodynamic parameters were calculated as follows:

$$In\, K_L = -\frac{\Delta H^0}{RT} + \frac{\Delta S^0}{R} \quad (7)$$

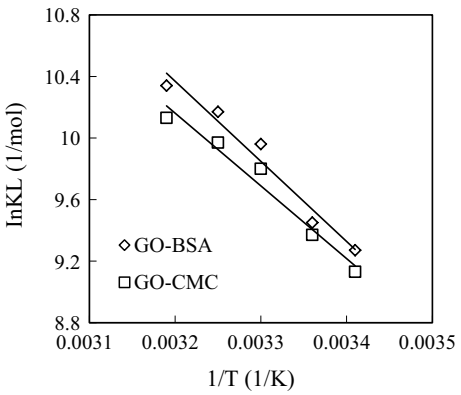

Fig. 8 Van't Hoff plots for the uptake of U(VI)

Table 4 Thermodynamic parameters for adsorption of U(VI) at different temperature

Sorbent	ΔH^0 (kJ mol^{-1})	ΔS^0 (J mol^{-1} K^{-1})	ΔG^0 (kJ mol^{-1})				
			293 K	298 K	303 K	308 K	313 K
GO-BSA	43.27	224.7	−22.57	−23.69	−24.81	−25.94	−27.06
GO-CMC	39.29	210.2	−22.30	−23.35	−24.4	−25.45	−26.50

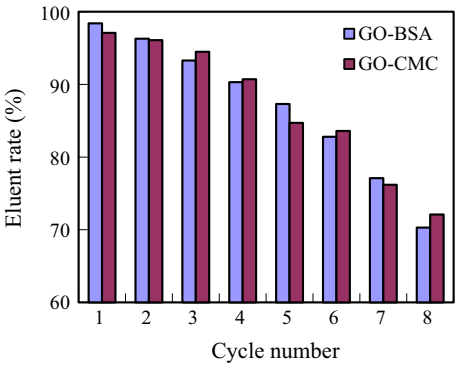

Fig. 9 Eluent rate with the cycle number of GO-BAS/CMC

$$\Delta G^0 = \Delta H^0 - T\Delta S^0 \quad (8)$$

where, R (8.314 J mol^{-1} K^{-1}) is the ideal gas constant, T is the adsorption temperature in Kelvin. K_L is the Langmuir constant in mL g^{-1}, respectively.

The slope and intercept of the Van't Hoff plots ($\ln K_d$ vs. $1/T$) shown in Fig. 8 give the values of ΔH^0 and ΔS^0, and the value of ΔG^0 was calculated from Eq. (8). The thermodynamic parameters obtained from the adsorption isotherms at pH 5.0 in the temperature range studied were listed in Table 4. The negative values of ΔG^0 indicate that these two adsorption processes are not only feasible but also spontaneous for GO-BSA/CMC, respectively. In our previous work [6], the ΔG^0 values becomes more negative with increasing temperature, indicating more favorable adsorption U(VI) at higher temperature. In addition, the positive values of ΔH^0 suggest the endothermic nature, while the positive ΔS^0 indicates the increase in the randomness of the sorption. These characteristics of thermodynamic parameters illustrates that GO-BAS/CMC can be used as two high-efficiency adsorbents to remove U(VI) from aqueous solution.

The regeneration of GO-BSA/CMC with practical method was performed to evaluate the renewability and reusability of the synthesized sorbent. It was found from the previous test that HNO_3 solution could efficiently desorb U(VI) from both GO-BSA and GO-CMC, therefore HNO_3 was used as the ideal eluent in this regeneration experiments. The adsorption processes were repeated 8 times, and the desorption efficiency of the exhausted adsorbent are shown in Fig. 9. The uptake capacities of U(VI) on the GO-BSA/CMC decreased slowly with increasing cycle number. The removal efficiency remained steady at 90% of the initial value for both GO-BSA and GO-CMC in the first four cycles, and then it decreased from the fifth cycle. At the last time regeneration cycles, the removal efficiency remained at 70%. Accordingly, the GO-BAS/CMC shows excellent reuse performance for U(VI) adsorption.

Conclusions

The present study reports the preparation and application of biopolymer/graphene oxide gels for the removal of U(VI) from aqueous solution. The obtained GO-BSA/CMC gels were thoroughly characterized using SEM, XRD, FTIR, and EDS, which showed the successful preparation of GO-BSA/CMC. The effects of pH of solution and contact time on adsorption process were investigated, and the optimum U(VI) adsorption conditions onto GO-BSA/CMC were found to be at pH of 5.0 and contact time of 120 min. The adsorption isotherms could be better described by Langmuir model compared to Freundlich model, demonstrating the homogeneous solid surface of the synthesized gels and the regular monolayer adsorption of U(VI). The adsorption kinetics data were described well by a pseudo-second-order kinetics model, indicating chemisorption of target analyte onto these adsorbents. The thermodynamics parameters suggested that the adsorption process of U(VI) on GO-BSA/CMC was endothermic and spontaneous.

Acknowledgements The present work was sponsored by the national science foundation of China (21866005) and the item of State Key Laboratory of Nuclear Resources and Environment (NRE 1611).

References

1. Liu SJ, Zhang HX, Peng DF, Yuan DZ, Wu LP, Ma JG (2017) Uranium uptake with grapheme oxide sponge prepared byfacile EDTA-assisted hydrothermal process. Int J Energy Res 41(2):263–273
2. Shao DD, Liu XH, Hayat T, Li JX, Re XM (2019) Poly(amidoxime) functionalized MoS_2 for efficient adsorption of uranium(VI) in aqueous solutions. J Radioanal Nucl Chem 319:379–386
3. Huang GL, Wi Peng, Yang SS (2018) Synthesis of magnetic chitosan/graphene oxide nanocomposites and its application for U(VI) adsorption from aqueous solution. J Radioanal Nucl Chem 317:337–344

4. Huang GL, Zou LX, Su Y, Lv TT, Wang LL (2016) Adsorption of uranium(VI) from aqueous solutions using cross-linked magnetic chitosan beads. J Radioanal Nucl Chem 307:1135–1140
5. Hu T, Ding SJ, Deng HJ (2016) Application of three surface complexation models on U(VI) adsorption onto graphene oxide. Chem Eng J 289:270-276
6. Zhou LM, Ouyang JB, Liu ZR, Huang GL, Wang Y, Li Z, Adesina AA (2019) Highly efficient sorption of U(VI) from aqueous solution using amino/amine-functionalized magnetic mesoporous silica nanospheres. J Radioanal Nucl Chem. https://doi.org/10.1007/s10967-018-6381-4
7. Zheng H, Zhou LM, Liu ZR, Le ZG, Ouyang JB, Huang GL, Shehzad H (2019) Functionalization of mesoporous Fe_3O_4@SiO_2 nanospheres for highly efficient U(VI) adsorption. Micropor Mesopor Mat 279:16–322
8. Mohamud H, Ivanov P, Russell BC, Regan PH, Ward NI (2018) Selective sorption of uranium from aqueous solution by graphene oxide-modified materials. J Radioanal Nucl Chem 316:839–848
9. Liu X, Li JX, Wang XX, Chen CL, Wang XK (2015) High performance of phosphate-functionalized graphene oxide for the selective adsorption of U(VI) from acidic solution. J Nucl Mater 466:56–64
10. Yang PP, Liu Q, Liu JY, Zhang HS, Li ZH, Li RM, Liu LH (2017) Bovine serum albumin-coated graphene oxide for effective adsorption of Uranium(VI) from aqueous solutions. Ind Eng Chem Res 56:3588–3598
11. Huang ZW, Li ZJ, Zheng LR, Zhou LM, Chai ZF, Wang XL, Shi WQ (2017) Interaction mechanism of uranium(VI) with three-dimensional grapheme oxide-chitosan composite: insights from batch experiments, IR, XPS, and EXAFS spectroscopy. Chem Eng J 328:1066–1074
12. Wang S, Ning HM, Hu N, Huang KY, Weng SY, Wu XP, Wu LK, Liu J, Alamusi S (2019) Preparation and characterization of graphene oxide/silk fibroin hybrid aerogel for dye and heavy metal adsorption. Compos B 163:716–722
13. Cheng CS, Deng J, Lei B, He A, Zhang X, Ma L, Li S, Zhao CS (2013) Toward 3D graphene oxide gels based adsorbents for high-efficient water treatment via the promotion of biopolymers. J Hazard Mater 263:467–478
14. Pan N, Li L, Ding J, Li S, Wang R, Jin Y, Wang X, Xia C (2016) Preparation of graphene oxide-manganese dioxide for highly efficient adsorption and separation of Th(IV)/U(VI). J Hazard Mater 309:107–115
15. Song W, Wang X, Wang Q, Shao D, Wang X (2015) Plasma-induced grafting of polyacrylamide on graphene oxide nanosheets for simultaneous removal of radionuclides. Phys Chem Chem Phys 17(1):398–406
16. Cheng HX, Zeng KF, Yu JT (2013) Adsorption of uranium from aqueous solution by graphene oxide nanosheets supported on sepiolite. J Radioanal Nucl Chem 298:599–603